

Article

A Facile Method for Preparing a Superhydrophobic Block with Rapid Reparability

Jiyuan Zhu * and Kaijin Liao

College of Mechanical and Control Engineering, Guilin University of Technology, Guilin 541004, China; KaijinLiao@163.com

* Correspondence: zhujiy@glut.edu.cn or zhujiyuanscut@163.com; Fax: +86-0773-3871-728

Received: 8 October 2020; Accepted: 8 December 2020; Published: 10 December 2020



Abstract: Superhydrophobic surfaces are fragile and are prone to failure in harsh outdoor environments. The preparation of robust superhydrophobic surfaces with stable performance and excellent properties can extend their application. In this paper, we report a simple and cost-effective method to prepare a superhydrophobic block using superhydrophobic zinc oxide powder and die pressing. The prepared sample has a contact angle of 163° and a sliding angle of 7° . Tests show that the superhydrophobic block can resist the impact of water flow, maintain its superhydrophobicity after friction or knife scraping, and quickly repair the destroyed surface by sandpaper abrasion. The sample exhibited excellent self-cleaning effect, robust mechanical property, and rapid reparability. This preparation method is also environmental-friendly and easy to operate. It will have a wide application prospect in many important fields.

Keywords: superhydrophobicity; block; rapid reparability; zinc oxide

1. Introduction

Inspired by many natural materials such as lotus leaves, roses, and water striders, scientists have developed water-repellent superhydrophobic surfaces that have a wide range of applications in different fields including self-cleaning [1,2] oil–water separation [3,4] drag reduction [5–7], corrosion resistance [8,9] water non-destructive transportation [10], and anti-icing [11–13]. With the deepening of research, the application of superhydrophobic surfaces has also been extended to the field of biopharmaceuticals [14,15]. Superhydrophobic surfaces will have great research and industrial value with the potential for large-scale industrial production. The general construction path of a superhydrophobic surface is to construct a rough structure on the surface of the substrate, and then use a low surface energy substance to modify the rough surface. Therefore, the chemical composition and surface structure are important factors that affect the surface wettability. In recent decades, common methods for preparing microstructures on surfaces include chemical etching [16,17], mechanical processing [18,19], chemical vapor deposition [20,21], femtosecond laser [22,23], and electrophoretic deposition [24,25]. In addition to these common methods, for example, Latthe et al. used a silica nanoparticle suspension to prepare superhydrophobic coatings on different substrates by simple dipping and spraying techniques [26]. Li et al. prepared a superhydrophobic/superlipophilic porous polycarbonate/carboxyl functionalized multiwalled carbon nanotube monolith with a new layered micro-nano structure by a thermally impacted nonsolvent induced phase separation method [27]. Marinaro et al. prepared a superhydrophobic chip by thin Si_3N_4 membranes with a tailored pattern of SU-8 photoresist pillars [28]. However, superhydrophobic surfaces have not been applied on a large scale in industry as expected. One factor contributing to this situation is that the preparation of superhydrophobic surfaces usually requires expensive processing equipment, complicated production processes, and the use of fluoropolymer-based modifiers that can cause hazards to the environment and human health.

Zinc oxide can be processed by different ways to produce a variety of morphologies such as hexagonal column [29], raspberry grain [30], and flower [31], etc., which is valuable for the study of surface wettability. Therefore, more and more scientists are trying to use ZnO as a material for preparing superhydrophobic surfaces. Due to the inherent hydrophilicity of ZnO, the general preparation method is to prepare ZnO with various morphologies through different methods and then modify the ZnO with low surface energy substances. Wu et al. prepared a ZnO nanorod-like microstructure surface through a wet chemical route and modified it with various alkanolic acids to obtain a superhydrophobic surface [32]. Qing et al. used stearic acid to modify ZnO and prepared a superhydrophobic coating on the surface of stainless steel by dip coating [33]. Sutha et al. prepared ZnO nanowalls on glass substrates by sonochemical technology, and then modified them with 1H, 1H, 2H, and 2H-perfluorooctyltrichlorosilane to obtain a superhydrophobic surface [34]. Wei et al. prepared a flower-like ZnO structure on a foamed nickel substrate through a hydrothermal and decomposition process, and then obtained a superhydrophobic surface by hydrophobic treatment of 1H, 1H, 2H, and 2H-perfluorooctyltrichlorosilane [35]. Although these methods all use ZnO to prepare various microstructures, they are easily damaged when used in harsh outdoor environments and are difficult to repair. In addition, the use of fluorine-containing modifiers is not only environmentally unfriendly, but also harmful to human health. Therefore, these methods for preparing superhydrophobic surfaces have certain limitations. As such, it is urgent to prepare environmentally friendly, robust, and easily repairable superhydrophobic surfaces to extend their application.

In this work, we present a simple and cost-effective method to prepare a superhydrophobic block with excellent mechanical durability and quick reparability. The hexagonal columnar ZnO powder was modified with stearic acid to change it from hydrophilic to hydrophobic, and then pressed by a mold to obtain a superhydrophobic block. Except for its excellent self-cleaning effect, tests showed both the external surface of the sample and the entire block obtained superhydrophobicity, so the sample had self-healing properties based on self-similarity. Once the microstructure formed by the hydrophobic ZnO particles stacked on each other is destroyed or fails, the internal microstructure can be exposed by friction to regain superhydrophobicity on the surface of the sample, which ensures the as-prepared sample good mechanical durability and rapid reparability. It will greatly cut the maintenance cost and extend the service life of the superhydrophobic surfaces under harsh conditions. This preparation method also has great advantage in its simple procedure and environmental-friendliness as it requires no sophisticated equipment nor any acidic or alkaline reagents. This approach will help to promote the practical applications of superhydrophobic surfaces in different important fields.

2. Materials and Method

2.1. Materials

The materials used in the experiment included commercial zinc oxide powder (Qinghe County Tuopu Metal Material Co., Ltd., Qinghe, China), $\text{CH}_3(\text{CH}_2)_{16}\text{COOH}$ (stearic acid), absolute ethanol, nylon mesh (600 mesh), and sandpaper (2000 mesh). The water used in the experiment was deionized water.

2.2. Method

A total of 0.65 g of stearic acid and 200 g of ethanol were added to a beaker, and a 3 wt.% stearic acid–ethanol solution was formed after stirring. Then, 30 g of zinc oxide powder was added to the stearic acid–ethanol solution, which was filtered with a nylon mesh after stirring with magnetic stirring for 5 h. The thick emulsion obtained after filtration was placed in an oven and dried at 75 °C until the emulsion became a block. The block was then crushed in a mortar and pressed to a cylindrical shape placed in a self-made mold (diameter 20 mm) to form a block. After the block was demolded, the surface layer of the block was removed with sandpaper to form a superhydrophobic surface.

2.3. Sample Characterization

The surface morphology of the sample was studied by scanning electron microscope (SEM, SU5000, Hitachi, Tokyo, Japan). The phase structure was analyzed by x-ray diffraction (XRD, Smartlab9, Rigaku Corporation, Tokyo, Japan). The chemical composition was analyzed by Fourier transform infrared spectroscopy (FTIR, Nicolet iS5, Thermofisher, Waltham, MA, USA). The static contact angle (CA) and sliding angle (SA) of the sample surface were measured by a contact angle measuring instrument (SDC-200, Sindin Precision Instrument Co., Ltd., Dongguan, China). The average contact angle was measured by 6 μ L of water droplets at six different positions on the sample surface.

3. Result and Discussion

3.1. Wettability

As shown in Figure 1a–c, the water droplets maintained a spherical shape on the prepared sample surface and the CA and SA of the sample surface were $163^\circ \pm 4^\circ$ and 7° , respectively, indicating that the sample surface obtained superhydrophobicity. Slow needle movement was used to measure the advancing contact angle (θ_a) and receiving contact angle (θ_r) of the sample surface. After the drop of water was dropped on the surface of sample, the needle tip was inserted into the center of the drop. The sample was moved slowly until the drop was about to move, and $\theta_a = 165.4^\circ$ and $\theta_r = 158.8^\circ$ were measured. Figure 1d shows that when the sample was placed in a beaker filled with water, a highly reflective surface with metallic luster appeared on the surface of the sample. Light is totally reflected on the surface of the sample. The superhydrophobic surface will trap a certain amount of air after being immersed in water as water and air are respectively light-dense medium and light-sparse medium, so the total reflection is achieved. As shown in Figure 1e–h, when a water droplet is dropped onto the surface of a block made of untreated ZnO powder, since the untreated ZnO is hydrophilic, the water droplet immediately diffuses to the surface of the block, and is then gradually absorbed by the block. Since the blocks made from untreated ZnO powder are hydrophilic, under the same conditions, the blocks made from the powder modified by stearic acid become superhydrophobic, so the hydrophobicity is formed by the modification of stearic acid. To study the effect of changing the content of stearic acid on the hydrophobic properties, 0.1, 0.2, 0.3, 0.4, and 0.5 wt.% stearic acid ethanol solutions were used to modify the ZnO particles under the same conditions. As shown in Figure 2, when the content of stearic acid was 0.1 wt.%, the CA of the sample surface was $141^\circ \pm 5^\circ$, and the sample exhibited hydrophobicity. When the content of stearic acid was increased to 0.2 wt.%, the CA of the sample surface was $153.6^\circ \pm 4^\circ$. When the stearic acid content was 0.3, 0.4, and 0.5 wt.%, the CA of the sample surface was $163^\circ \pm 2^\circ$, $163.5^\circ \pm 3^\circ$, and $161.1^\circ \pm 3^\circ$, respectively. The sample surface exhibited superhydrophobicity. Therefore, the use of 3 wt.% stearic acid solution can make the sample use less modifier to obtain better hydrophobic properties.

The water adhesion of the sample surface can be evaluated by the bouncing test of water droplets. As shown in Figure 3a–f, a needle tube was used to drip a water droplet 30 mm away from the surface of the sample, and a bouncing test was performed on the sample surface. Under the influence of gravity, the water droplet soon reached the surface of the sample in a pie shape, then left the surface of the sample under the reaction force with the sample surface, and finally fell to the sample surface again. When the water droplet landed on the surface, it bounced off and left the surface. The test result showed that the water droplet had a strong bouncing ability on the sample, which can be due to a low viscosity of the sample surface to water and its better superhydrophobicity.

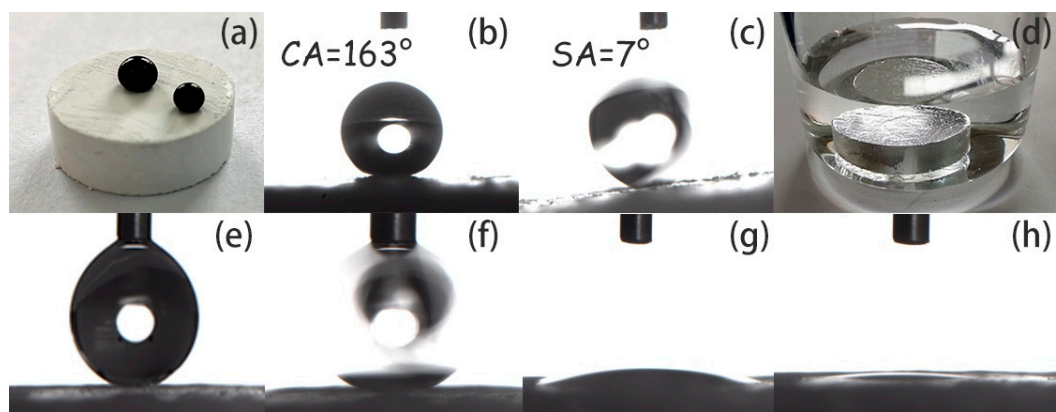


Figure 1. (a) Digital image of a water droplet containing ink on the sample surface. (b) Contact angle (CA) of the sample surface. (c) Sliding angle (SA) of the sample surface. (d) Digital photo of the sample in water. (e–h) Digital image of a water droplet touching a block made of untreated ZnO powder.

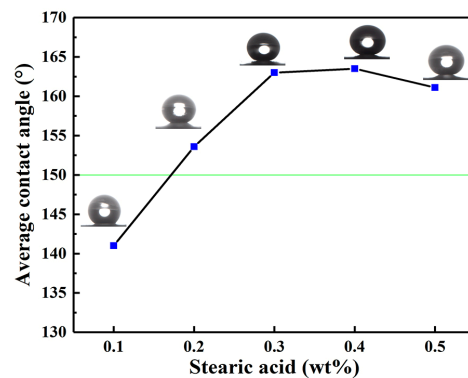


Figure 2. The effect of stearic acid content on contact angle.

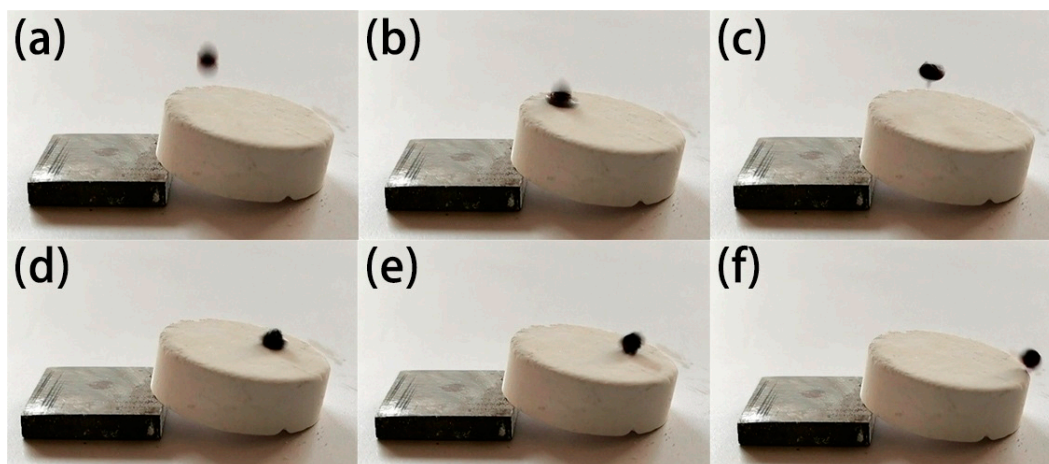


Figure 3. (a–f) Digital photo of water drop bouncing on the superhydrophobic surface.

3.2. Surface Morphology

The formation of a superhydrophobic surface is the result of the combined effect of chemical composition and surface structure. Therefore, the general method of preparing a superhydrophobic surface is to prepare a rough structure on the substrate and then modify it with a substance with low surface energy. In this work, we first modified ZnO to change it from hydrophilic to hydrophobic, and then combined the ZnO particles to form a rough structure through the pressing of the mold. The surface morphology of the prepared samples was studied by scanning electron microscopy (SEM)

images with different magnifications. As shown in Figure 4a,b, the surface of the sample was rough, hence many voids formed on the surface of the sample. The voids can trap more air, which is beneficial to the improvement of hydrophobicity. The structure of the sample surface is further studied by observing images with higher magnification. As shown in Figure 4c,d, the surface of the sample was composed of structures on different scales. The first structures were zinc oxide particles, which had a large size and a length of about 1.5 μm , and their shapes were mainly irregular. The second structures were the ZnO nanorods growing on the surface of the ZnO particles. These nanorods were bar-shaped with a hexagonal crystal plane and the length was about 300 nm. These nanorods covered the surface of ZnO particles in large quantities and formed micro/nano structures together with ZnO particles, which is beneficial to the improvement of the hydrophobicity of the surface.

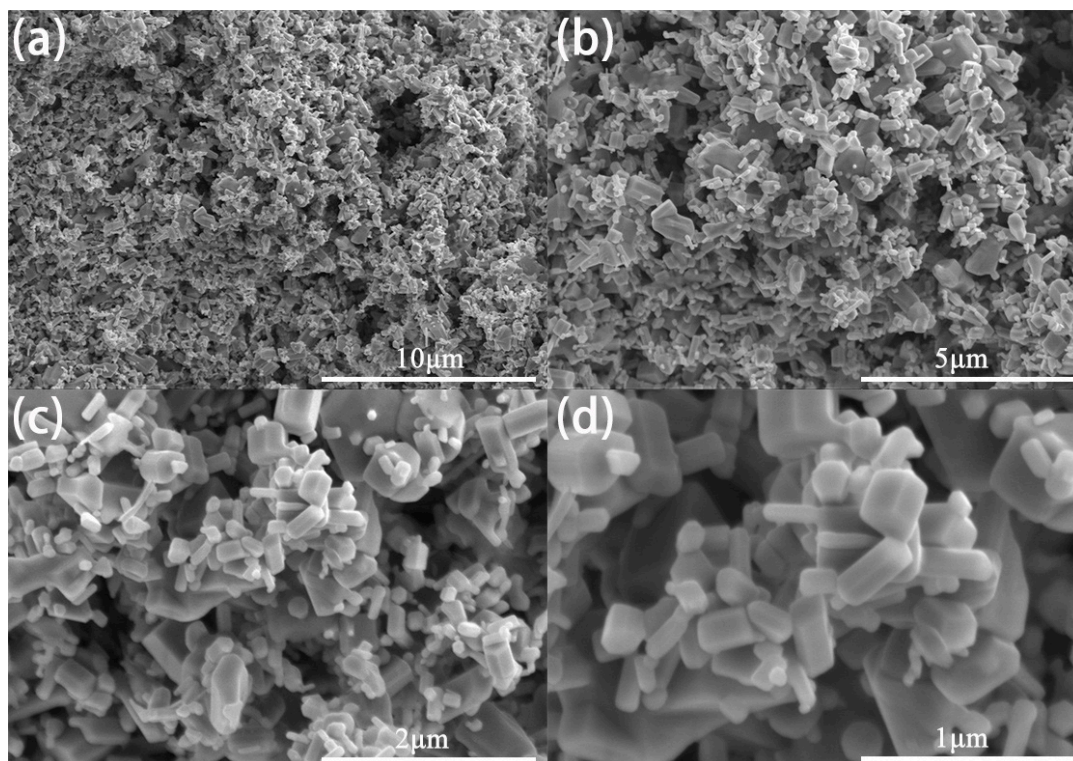


Figure 4. Scanning electron microscopy (SEM) images of the sample at different magnifications. (a) 5k, (b) 10k, (c) 25k, (d) 50k.

3.3. Chemical Composition

For phase analysis of the superhydrophobic surface, the sample was tested using an x-ray diffractometer. Figure 5 is the XRD pattern of the superhydrophobic surface, and the scanning range of the test was in the range of $2\theta = 10^\circ\text{--}80^\circ$. Sharp diffraction peaks appeared at 2θ angles of 31.8° , 34.4° , 36.3° , 47.5° , 56.6° , 62.8° , 66.3° , 67.9° , 69.1° , 72.6° , and 76.9° , corresponding to (100), (002), (101), (102), (110), (103), (200), (112), (201), (004), and (202) crystal planes, respectively. The diffraction peaks obtained from the test were consistent with the results of the ZnO x-ray diffraction standard card (PDF#36-1451). The strong diffraction peaks at 31.8° , 34.4° , and 36.3° indicate that the ZnO powder used in this study had a hexagonal crystal phase. The average particle size of ZnO was calculated by the Scherrer equation. To remove the influence of instrument broadening, the intrinsic width curve of the instrument was obtained by scanning LaB6 powder. Scherrer constant $K = 1$. The average particle size of ZnO used in this study was 156 nm. The reaction mechanism of zinc oxide modified by stearic acid is shown in Figure 6. The hydroxyl ($-\text{OH}$) on the surface of ZnO reacts with the carboxyl ($-\text{COOH}$) of stearic acid, and the hydrophilic $-\text{OH}$ on the surface of ZnO is replaced by the non-polar hydrophobic alkane in the stearic acid, making ZnO change from hydrophilic to hydrophobic. Figure 7

is the FTIR spectrum of stearic acid powder and superhydrophobic surface. The chemical composition of the superhydrophobic surface can be studied by the FTIR spectrum. As shown in Figure 7, the strong and broad absorption peak of the sample at 434 cm^{-1} can be attributed to the vibration of the Zn–O framework. The absorption peak of the sample at 3418 cm^{-1} can be attributed to the stretching vibration of –OH. The absorption peak of stearic acid at 1700 cm^{-1} was assigned to the stretching vibration of –COOH. After the reaction between stearic acid and ZnO, stearic acid exists in the form of carboxylate (COO–) on the surface of ZnO, so the sample had a COO– absorption peak at 1541 cm^{-1} . In addition, the absorption peaks of the samples and stearic acid powder at wavelengths of 2847 and 2917 cm^{-1} were attributed to the antisymmetric and symmetric stretching vibrations of the methylene group (–CH₂) and methyl group (–CH₃) [36].

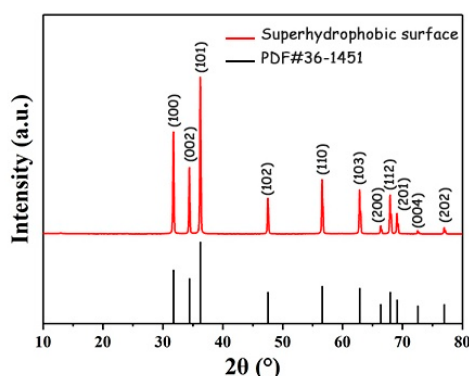


Figure 5. X-ray diffraction (XRD) pattern of the prepared sample.

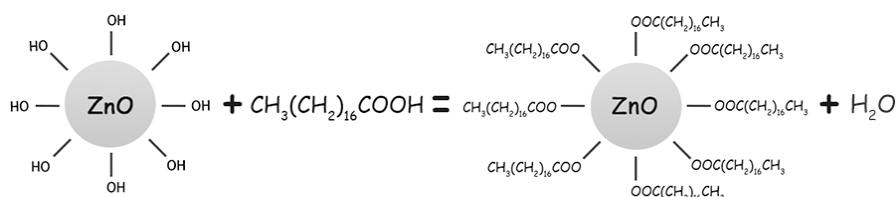


Figure 6. Diagram of the reaction mechanism of zinc oxide and stearic acid.

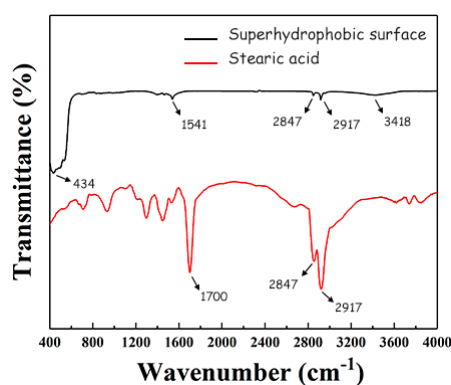


Figure 7. Fourier transform infrared (FTIR) spectrum of the prepared sample.

3.4. Self-Cleaning Effect

The self-cleaning effect is one of the most important capabilities of superhydrophobic surfaces. To test the self-cleaning performance of the samples, a layer of chalk dust was sprinkled on the surface of the samples to perform the self-cleaning test [37,38]. As shown in Figure 8a–f, a needle was used to drop a water drop on the surface of the sample covered with chalk dust. When the water drop falls on the surface of the sample, it rolls forward along the surface of the sample under the influence of gravity. During the rolling of the water droplets, since the chalk ash is hydrophilic, the chalk ash is

absorbed by the water droplets and then leaves the surface of the sample along with the rolling water droplets. As the number of dripping water drops continues to increase, the chalk dust on the rolling path of the water drops is easily removed. The test results showed that the prepared samples had an excellent self-cleaning effect.

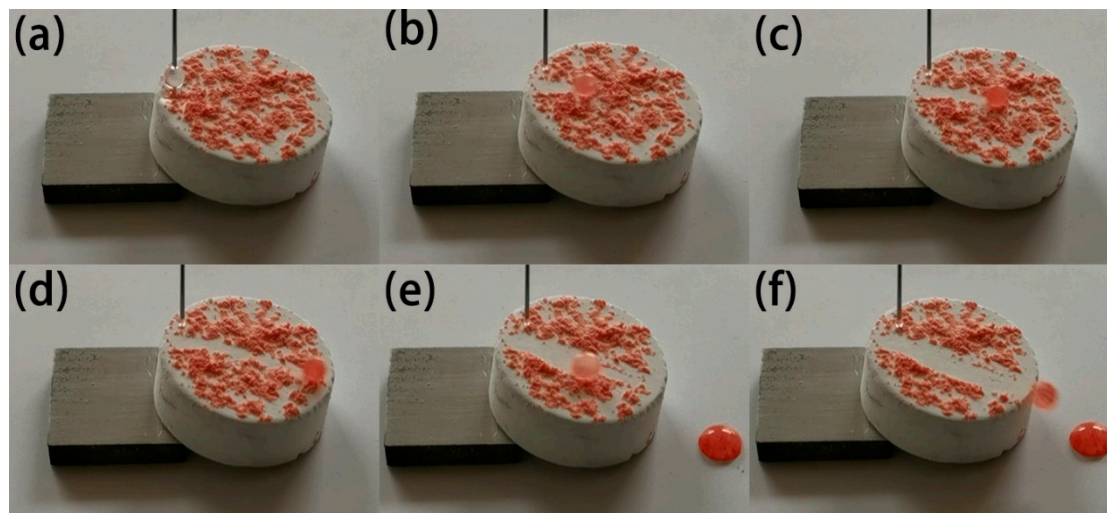


Figure 8. (a–f) Self-cleaning test of chalk ash.

3.5. Durability

People have been working hard to improve the mechanical robustness of superhydrophobic surfaces [39–41], so mechanical robustness is an important criterion for measuring the performance of superhydrophobic surfaces. Durability tests were performed on the prepared samples. As shown in Figure 9a, the resistibility of the sample to the impact of the water flow was tested by spraying a water flow on the sample surface through a needle tube. When the water flow reached the surface of the sample from the needle tube, the water flow reflected like light on the surface. This phenomenon indicates that the impact of water flow neither damages the sample surface nor changes the wettability of the sample surface.

The ability to resist scratches and friction is an important criterion for whether the superhydrophobic surface can be put into practical application. To study the stability of the sample, the sample was subjected to the friction test and knife scraping. Use 360-mesh sandpaper to continuously rub one side of the sample surface until both sides of the sample surface are stepped, exposing the inner surface. At this time, the water droplets maintain a spherical shape on the inner surface and the CA is $164.7^\circ \pm 3^\circ$. As shown in Figure 9b, the water droplet retained a spherical shape on both the unrubbed surface (right) and the rubbed surface (left), respectively. This indicates that the interior of the sample and its external surface are coherent. Both are superhydrophobic. In Figure 9c, the sample was scraped by a knife. It can be seen from Figure 9d that water droplets rolled off the surface being scraped, suggesting that if the surface of the block is damaged, the sample still exhibited superhydrophobicity and the CA was $161.1^\circ \pm 4^\circ$.

In practical applications, the superhydrophobic surface was easily contaminated by oil. When a certain amount of oil remains on the superhydrophobic surface, the sample surface will fail. As shown in Figure 9e, to verify the rapid reparability of the sample, the sample was tested for oil contamination. A drop of silicone oil was dropped onto the surface of the sample. Due to the low surface tension of the silicone oil, the silicone oil immediately penetrated into the sample. Wiping off the silicone oil on the surface, the CA of the water drop on the sample surface was $122^\circ \pm 7^\circ$, which means that the superhydrophobicity of the sample surface is lost. As shown in Figure 9f, after removing the contaminated surface with sandpaper, the CA of the water droplets on the surface of the sample increased to $166^\circ \pm 3^\circ$, which shows that after rapid reparability of the sample by abrasion, the sample restored superhydrophobicity.

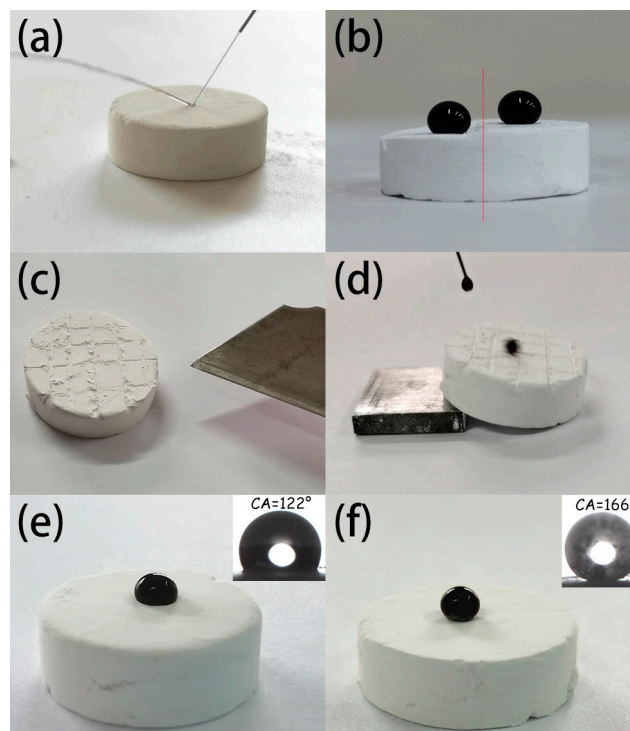


Figure 9. (a) Water jet reflection on the superhydrophobic surface. (b) Digital photo of water drops on the surface before and after abrasion. (c) Digital image of sample scraped by knife. (d) Water droplets are rolling off the surface of the sample being scraped. (e) Water droplet on the surface of the sample after being contaminated with oil. Inset shows the CA of the contaminated surface is 122° . (f) Water droplets on the repaired sample surface. Inset shows the CA of the water droplet on the repaired surface was 166° .

To study the effect of different pH on the sample surface, water droplets with different pH were dropped on the sample surface and the CA was measured. As shown in Figure 10a, the water droplets with pH values of 1, 3, 5, 7, 10, 12, and 14 maintained a spherical shape on the surface of the sample. As shown in Figure 10b, the CA of the droplet with a pH of 14 was 159.2° when it was dropped on the surface of the sample. After 2 min, the CA of the droplet dropped to 150.3° , and after 4 min, the CA of the droplet was 147.2° . When the pH value of the droplet changed from 14 to 1, as shown in Figure 10c, the CA of the droplet was 160.9° when it was dropped on the surface of the sample. After 3 min, the CA dropped to 150.6° , and after 5 min, the CA of the droplet was 144.3° .

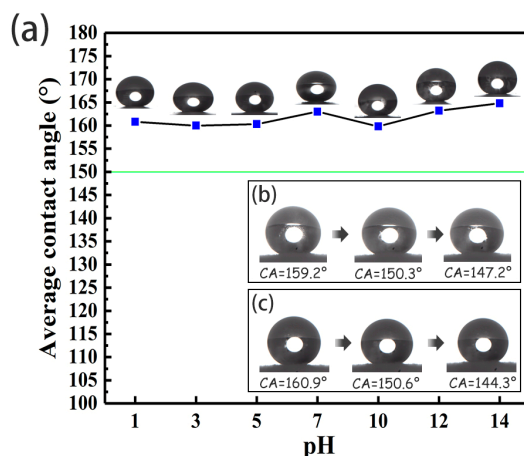


Figure 10. (a) The contact angle of water droplets with different pH values on the sample surface. (b) The change of the contact angle of water droplets with a pH of 14 over time. (c) The change of the contact angle of water droplets with a pH of 1 over time.

4. Conclusions

In this study, we proposed a method for preparing a robust superhydrophobic block by superhydrophobic zinc oxide powder, and the resulting surface had a CA and SA of 163° and 7°, respectively. The prepared block had excellent self-cleaning properties, and could easily remove contaminants on the surface through water droplets. The samples exhibited self-similarity and maintained excellent water repellency even after water impact, friction, and knife scraping. It is worth noting that superhydrophobicity was achieved on the entire block. Once the surface of the sample fails, the surface can be removed by sandpaper to make the sample easily and quickly restore superhydrophobicity. The preparation method of the superhydrophobic block is facile and does not need complex equipment and fluorinated materials, which is conducive to mass industrial production. Therefore, superhydrophobic blocks with great mechanical durability and rapid repairability will have great industrial value.

Author Contributions: Conceptualization, J.Z.; Investigation, K.L.; Methodology, J.Z.; Software, K.L.; Writing—original draft, K.L.; Writing—review & editing, J.Z. All authors have read and agreed to the published version of the manuscript.

Funding: This research received no external funding.

Conflicts of Interest: The authors declare no conflict of interest.

References

- Guo, Z.; Liu, W.; Su, B. Superhydrophobic surfaces: From natural to biomimetic to functional. *J. Colloid Interface Sci.* **2011**, *353*, 335–355.
- Ueda, E.; Levkin, P. Emerging applications of superhydrophilic-superhydrophobic micropatterns. *Adv. Mater.* **2013**, *25*, 1234–1247. [[CrossRef](#)] [[PubMed](#)]
- Chu, Z.; Feng, Y.; Seeger, S. Oil/water separation with selective superantiwetting/superwetting surface materials. *Angew. Chem. Int. Ed.* **2015**, *54*, 2328–2338. [[CrossRef](#)]
- Xue, Z.; Cao, Y.; Liu, N.; Feng, L.; Jiang, L. Special wettable materials for oil/water separation. *J. Mater. Chem. A* **2014**, *2*, 2445–2460. [[CrossRef](#)]
- Aljallis, E.; Sarshar, M.A.; Datla, R.; Sikka, V.; Jones, A.; Choi, C.-H. Experimental study of skin friction drag reduction on superhydrophobic flat plates in high Reynolds number boundary layer flow. *Phys. Fluids* **2013**, *25*, 025103. [[CrossRef](#)]
- Dong, H.; Cheng, M.; Zhang, Y.; Wei, H.; Shi, F. Extraordinary drag-reducing effect of a superhydrophobic coating on a macroscopic model ship at high speed. *J. Mater. Chem. A* **2013**, *1*, 5886–5891. [[CrossRef](#)]

7. Liu, Y.; Gu, H.; Jia, Y.; Liu, J.; Zhang, H.; Wang, R.; Zhang, B.; Zhang, H.; Zhang, Q. Design and preparation of biomimetic polydimethylsiloxane (PDMS) films with superhydrophobic, self-healing and drag reduction properties via replication of shark skin and SI-ATRP. *Chem. Eng. J.* **2019**, *356*, 318–328. [[CrossRef](#)]
8. Qian, H.; Xu, D.; Du, C.; Zhang, D.; Li, X.; Huang, L.; Deng, L.; Tu, Y.; Mol, J.; Terryn, H.A. Dual-action smart coatings with a self-healing superhydrophobic surface and anti-corrosion properties. *J. Mater. Chem. A* **2017**, *5*, 2355–2364. [[CrossRef](#)]
9. Vazirinasab, E.; Jafari, R.; Momen, G. Application of superhydrophobic coatings as a corrosion barrier: A review. *Surf. Coat. Technol.* **2018**, *341*, 40–56. [[CrossRef](#)]
10. Ben, S.; Zhou, T.; Ma, H.; Yao, J.; Ning, Y.; Tian, D.; Liu, K.; Jiang, L. Multifunctional magnetocontrollable superwetable microcilia surface for directional droplet manipulation. *Adv. Sci.* **2019**, *6*, 1900834. [[CrossRef](#)]
11. Jiang, G.; Chen, L.; Zhang, S.; Huang, H.-X. Superhydrophobic SiC/CNTs coatings with photothermal deicing and passive anti-icing properties. *ACS Appl. Mater. Interfaces* **2018**, *10*, 36505–36511. [[CrossRef](#)] [[PubMed](#)]
12. Lin, Y.; Chen, H.; Wang, G.; Liu, A. Recent progress in preparation and anti-icing applications of superhydrophobic coatings. *Coatings* **2018**, *8*, 208. [[CrossRef](#)]
13. Peng, C.; Xing, S.; Yuan, Z.; Xiao, J.; Wang, C.; Zeng, J. Preparation and anti-icing of superhydrophobic PVDF coating on a wind turbine blade. *Appl. Surf. Sci.* **2012**, *259*, 764–768. [[CrossRef](#)]
14. Renard, C.; Leclercq, L.; Stocco, A.; Cottet, H. Superhydrophobic capillary coatings: Elaboration, characterization and application to electrophoretic separations. *J. Chromatogr. A* **2019**, *1603*, 361–370. [[CrossRef](#)] [[PubMed](#)]
15. Zhong, H.; Zhu, Z.; You, P.; Lin, J.; Cheung, C.F.; Lu, V.L.; Yan, F.; Chan, C.-Y.; Li, G. Plasmonic and superhydrophobic self-decontaminating N95 respirators. *ACS Nano* **2020**, *14*, 8846–8854. [[CrossRef](#)]
16. Gupta, N.; Sasikala, S.; Barshilia, H.C. Corrosion study of superhydrophobic magnesium alloy AZ31 surfaces prepared by wet chemical etching process. *Nanosci. Nanotechnol. Lett.* **2012**, *4*, 757–765. [[CrossRef](#)]
17. Kumar, A.; Gogoi, B. Development of durable self-cleaning superhydrophobic coatings for aluminium surfaces via chemical etching method. *Tribol. Int.* **2018**, *122*, 114–118. [[CrossRef](#)]
18. Zhu, J. A novel fabrication of superhydrophobic surfaces on aluminum substrate. *Appl. Surf. Sci.* **2018**, *447*, 363–367. [[CrossRef](#)]
19. Zhu, J.; Hu, X. A new route for fabrication of the corrosion-resistant superhydrophobic surface by milling process. *J. Coat. Technol. Res.* **2019**, *16*, 249–255. [[CrossRef](#)]
20. Crick, C.R.; Bear, J.C.; Kafizas, A.; Parkin, I.P. Superhydrophobic photocatalytic surfaces through direct incorporation of titania nanoparticles into a polymer matrix by aerosol assisted chemical vapor deposition. *Adv. Mater.* **2012**, *24*, 3505–3508. [[CrossRef](#)]
21. Zhang, F.; Shi, Z.; Chen, L.; Jiang, Y.; Xu, C.; Wu, Z.; Wang, Y.; Peng, C. Porous superhydrophobic and superoleophilic surfaces prepared by template assisted chemical vapor deposition. *Surf. Coat. Technol.* **2017**, *315*, 385–390. [[CrossRef](#)]
22. Long, J.; Fan, P.; Gong, D.; Jiang, D.; Zhang, H.; Li, L.; Zhong, M. Superhydrophobic surfaces fabricated by femtosecond laser with tunable water adhesion: From lotus leaf to rose petal. *ACS Appl. Mater. Interfaces* **2015**, *7*, 9858–9865. [[CrossRef](#)] [[PubMed](#)]
23. Song, Y.; Wang, C.; Dong, X.; Yin, K.; Zhang, F.; Xie, Z.; Chu, D.; Duan, J. Controllable superhydrophobic aluminum surfaces with tunable adhesion fabricated by femtosecond laser. *Opt. Laser Technol.* **2018**, *102*, 25–31. [[CrossRef](#)]
24. Ogihara, H.; Katayama, T.; Saji, T. One-step electrophoretic deposition for the preparation of superhydrophobic silica particle/trimethylsiloxysilicate composite coatings. *J. Colloid Interface Sci.* **2011**, *362*, 560–566. [[CrossRef](#)] [[PubMed](#)]
25. Xu, Z.; Jiang, D.; Wei, Z.; Chen, J.; Jing, J. Fabrication of superhydrophobic nano-aluminum films on stainless steel meshes by electrophoretic deposition for oil-water separation. *Appl. Surf. Sci.* **2018**, *427*, 253–261. [[CrossRef](#)]
26. Latthe, S.S.; Sutar, R.S.; Kodag, V.S.; Bhosale, A.; Kumar, A.M.; Sadasivuni, K.K.; Xing, R.; Liua, S. Self-cleaning superhydrophobic coatings: Potential industrial applications. *Prog. Org. Coat.* **2019**, *128*, 52–58. [[CrossRef](#)]
27. Li, Z.; Wang, B.; Qin, X.; Wang, Y.; Liu, C.; Shao, Q.; Wang, N.; Zhang, J.; Wang, Z.; Shen, C.; et al. Superhydrophobic/superoleophilic polycarbonate/carbon nanotubes porous monolith for selective oil adsorption from water. *ACS Sustain. Chem. Eng.* **2018**, *6*, 13747–13755. [[CrossRef](#)]

28. Marinaro, G.; Accardo, A.; De Angelis, F.; Dane, T.; Weinhausen, B.; Burghammer, M.; Riekkel, C. A superhydrophobic chip based on SU-8 photoresist pillars suspended on a silicon nitride membrane. *Lab Chip* **2014**, *14*, 3705–3709. [[CrossRef](#)]
29. Si, W.; Yu, J.; Huang, M.; Ding, C.; Gao, H. Controllable synthesis and photocatalytic activities of cube and hexagonal prism ZnO. *Micro Nano Lett.* **2012**, *7*, 1324–1327. [[CrossRef](#)]
30. Ding, N.; Sun, Y.; Chen, B.; Wang, D.; Tao, S.; Zhao, B.; Li, Y. Facile preparation of raspberry-like PS/ZnO composite particles and their antibacterial properties. *Colloids Surf. A Physicochem. Eng. Asp.* **2020**, *599*, 124867. [[CrossRef](#)]
31. Shi, R.; Yang, P.; Dong, X.; Ma, Q.; Zhang, A. Growth of flower-like ZnO on ZnO nanorod arrays created on zinc substrate through low-temperature hydrothermal synthesis. *Appl. Surf. Sci.* **2013**, *264*, 162–170. [[CrossRef](#)]
32. Wu, X.; Zheng, L.; Wu, D. Fabrication of superhydrophobic surfaces from microstructured ZnO-based surfaces via a wet-chemical route. *Langmuir* **2005**, *21*, 2665–2667. [[CrossRef](#)]
33. Qing, Y.-Q.; Yang, C.-N.; Sun, Y.-Z.; Zheng, Y.-S.; Shang, Y.; Liu, C. Simple method for preparing ZnO superhydrophobic surfaces with micro/nano roughness. *J. Adhes. Sci. Technol.* **2015**, *29*, 2153–2159. [[CrossRef](#)]
34. Sutha, S.; Kumar, R.T.R.; Raj, B.; Ravi, K.R. Ultrasonic-assisted fabrication of superhydrophobic ZnO nanowall films. *Bull. Mater. Sci.* **2017**, *40*, 505–511. [[CrossRef](#)]
35. Wei, X.-L.; Li, N.; An, J.-F.; Huo, C.-F.; Liu, H.; Yang, R.; Li, X.; Chao, Z.-S. Synthesis of superhydrophobic flower-like ZnO on nickel foam. *CrystEngComm* **2020**, *22*, 205–212. [[CrossRef](#)]
36. Zhu, W.; Wu, Y.; Zhang, Y. Fabrication and characterization of superhydrophobicity ZnO nanoparticles with two morphologies by using stearic acid. *Mater. Res. Express* **2019**, *6*, 1150d1. [[CrossRef](#)]
37. Banerjee, S.; Dionysiou, D.D.; Pillai, S.C. Self-cleaning applications of TiO₂ by photo-induced hydrophilicity and photocatalysis. *Appl. Catal. B Environ.* **2015**, *396*–428. [[CrossRef](#)]
38. Bhushan, B.; Jung, Y.C. Natural and biomimetic artificial surfaces for superhydrophobicity, self-cleaning, low adhesion, and drag reduction. *Prog. Mater. Sci.* **2011**, *56*, 1–108. [[CrossRef](#)]
39. Milionis, A.; Loth, E.; Bayer, I.S. Recent advances in the mechanical durability of superhydrophobic materials. *Adv. Colloid Interface Sci.* **2016**, *229*, 57–79. [[CrossRef](#)]
40. Masood, M.T.; Zahid, M.; Goldoni, L.; Ceseracciu, L.; Athanassiou, A.; Bayer, I.S. Highly transparent polyethylcyanoacrylates from approved eco-friendly fragrance materials demonstrating excellent fog-harvesting and anti-wear properties. *ACS Appl. Mater. Interfaces* **2018**, *10*, 34573–34584. [[CrossRef](#)]
41. Bayer, I.S. On the durability and wear resistance of transparent superhydrophobic coatings. *Coatings* **2017**, *7*, 12. [[CrossRef](#)]

Publisher's Note: MDPI stays neutral with regard to jurisdictional claims in published maps and institutional affiliations.



© 2020 by the authors. Licensee MDPI, Basel, Switzerland. This article is an open access article distributed under the terms and conditions of the Creative Commons Attribution (CC BY) license (<http://creativecommons.org/licenses/by/4.0/>).